Csizmadia et al., https://doi.org/10.1083/jcb.201702145

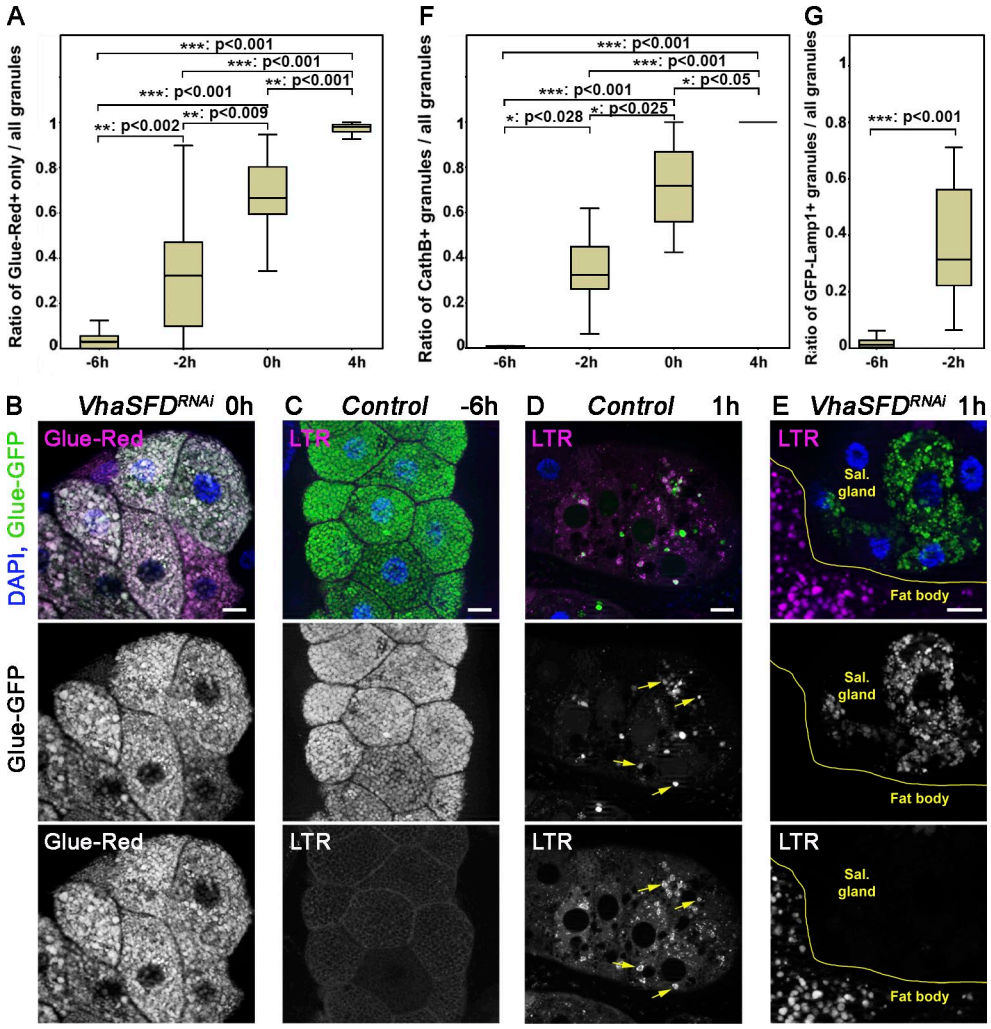


Figure S1. **The effect of v-ATPase loss on glue degradation, and statistical analysis of developmental crinophagy.** (A) Quantification of crinophagy progression data shown in Fig. 1 (A–D) based on the Glue-Flux reporter system; *n* = 30–41 cells. (B) Knockdown of *VhaSFD* encoding a subunit of the v-ATPase proton pump prevents the lysosomal quenching of GFP in white prepupae (compare Fig. 1 C). (C–E) Lysotracker red (LTR) data. No acidic vesicles are detected in −6 h RPF glands, whereas many punctate structures are seen that colocalize with Glue-GFP (arrows) in salivary gland cells of 1 h RPF animals (D). Salivary gland–specific RNAi silencing of *VhaSFD* prevents LTR staining of Glue-GFP granules in similarly aged cells (E). Please note that the adjacent fat body is shown as a positive control for LTR positivity. Green and magenta channels are shown separately as indicated. Bars, 20 µm. (F) Quantification of crinophagy progression data shown in Fig. 1 (E–H) based on the Glue-GFP, CathB-3xmCherry reporter system; *n* = 15–33 cells. (G) Quantification of crinophagy progression data shown in Fig. 1 (I and J) based on the Glue-Red, GFP-Lamp1 reporter system; *n* = 15 cells. In statistical analyses, Kruskal–Wallis tests with post-hoc *U* test (A and F) or Mann–Whitney *U* test (G) was used to compare samples. In the box plots, bars show the data ranging between the upper and lower quartiles, and median is indicated as a horizontal black line within the box. Whiskers plot the smallest and largest observations.

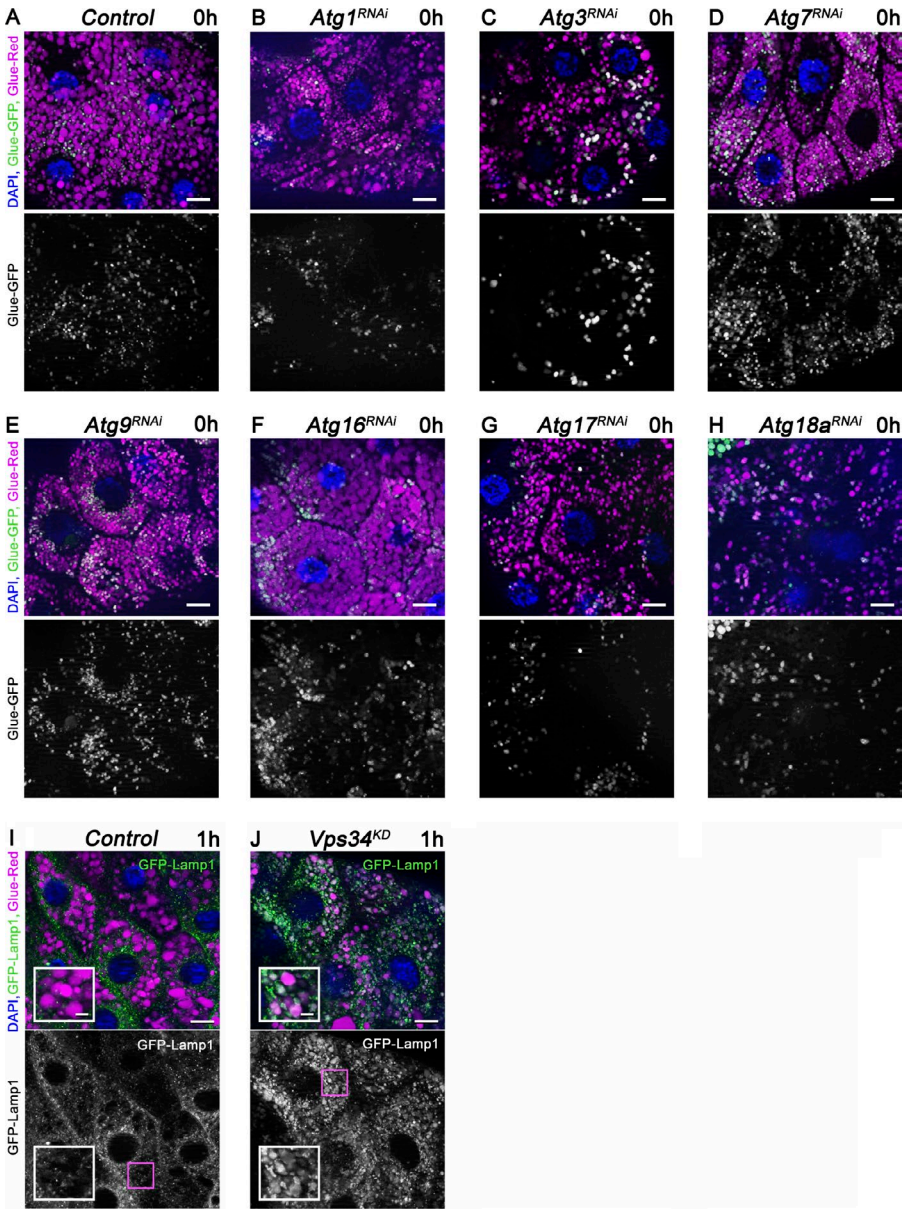


Figure S2. **Core macroautophagy genes are dispensable for the degradation of glue granules.** (A–H) Knockdown of the core macroautophagy genes *Atg1* (B), *Atg3* (C), *Atg7* (D), *Atg9* (E), *Atg16* (F), *Atg17* (G), or *Atg18a* (H) does not influence the quenching of Glue-GFP in salivary gland cells of white prepupae compared with controls (A). (I and J) Inhibition of Vps34 causes accumulation of GFP-Lamp1 within the lumen of crinosomes in 1 h RPF animals (J), unlike in controls, where crinosomal GFP signal has already been quenched at this stage (I). Boxed regions in I and J are shown enlarged in insets, respectively. Green channels are shown separately in A–J. Bars: (A–J) 20 µm; (I and J, insets) 3 µm.

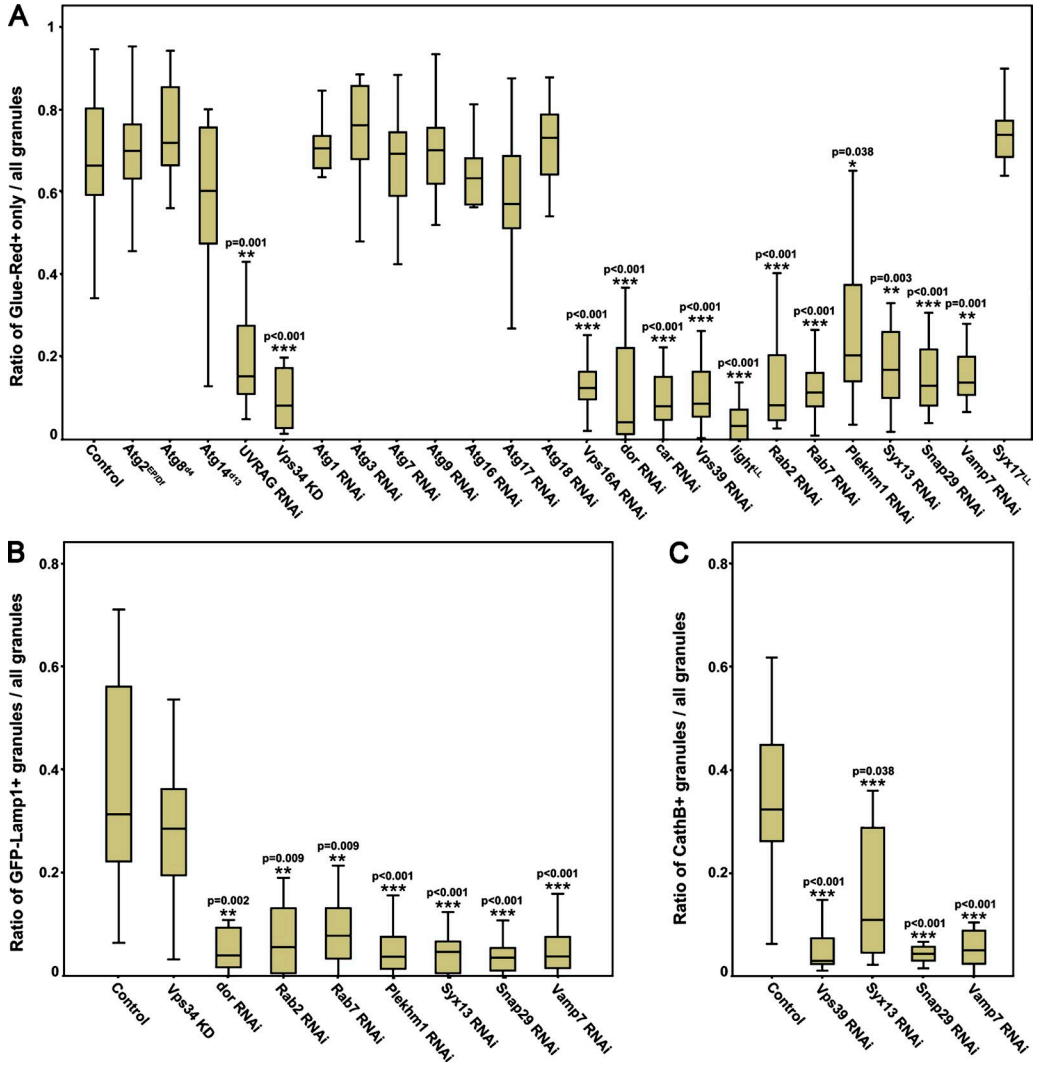


Figure S3. **Quantification of crinophagy in different genetic backgrounds.** (A) Quantification of crinophagy in white prepupal glands shown in Figs. 2 (A–F), S2 (A–H), 3 (A–F), 5 (A–D), 6 (A–D), and S5 B, based on the Glue-Flux reporter system; *n* = 15–36 cells. (B) Quantification of crinosome formation in −2 h RPF glands shown in Figs. 2 (G and H), 3 (G and H), 5 (E–H), and 6 (I–L) based on the Glue-Red, GFP-Lamp1 reporter system; *n* = 15–21 cells. (C) Quantification of crinosome formation shown in Figs. 3 (I and J) and 6 (E–H), based on the Glue-GFP, CathB-3xmCherry reporter system; *n* = 12–30 cells. The overlap of Glue-GFP with CathB is strongly reduced in cells undergoing *Vps39*, *Snap29*, and *Vamp7* RNAi and to a smaller extent by *Syx13* knockdown (KD). In statistical analyses for A–C, Kruskal–Wallis tests with a post-hoc *U* test were used to compare samples. In the box plots, bars show the data ranging between the upper and lower quartiles; median is indicated as a horizontal black line within the box. Whiskers plot the smallest and largest observations.

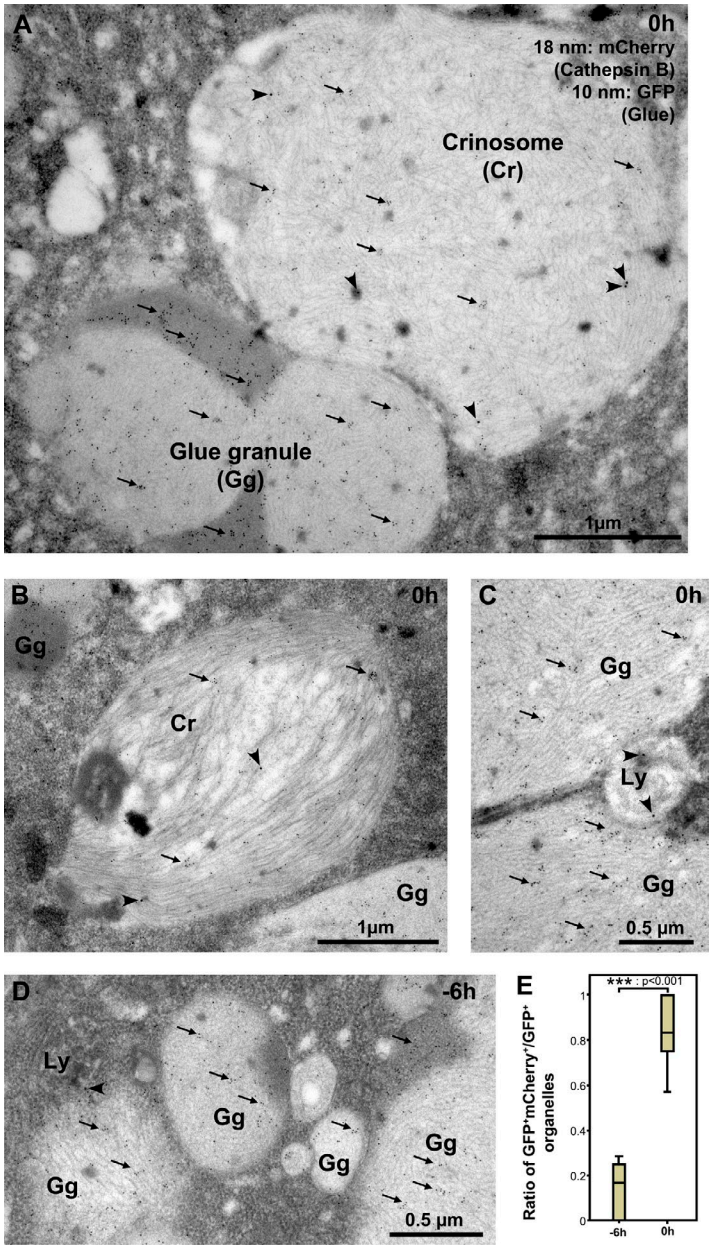


Figure S4. **Identification of intact glue granules, lysosomes, and crinosomes in salivary gland cells using immunogold labeling.** (A–D) Immuno-EM labeling of Glue-GFP (10 nm gold) and CathB-3xmCherry (18 nm gold). (A) At 0 h RPF, both intact glue granules (Gg) and crinosomes (Cr) are heavily labeled with anti-GFP, as expected, because both contain Glue-GFP. Note that 10-nm gold particles are in highest density in the electron-dense region of intact granules, and crinosomes contain relatively fewer gold particles. Crinosomes are less electron dense than glue granules, with their contents appearing loose, and they are identified by the presence of CathB-3xmCherry detected by 18-nm gold particles. (B) This panel shows a crinosome positive for both 10-nm (glue) and 18-nm (CathB) gold particles, and parts of two intact granules containing only glue. (C) A small CathB-positive, glue-negative lysosome is seen attached to two glue granules. (D) A CathB-positive lysosome is located near intact glue granules in a −6 h RPF cell. 10-nm gold particles are marked by arrows, and 18-nm gold particles are highlighted by arrowheads in A–D. (E) Quantification of the ratio of GFP-positive mCherry double-positive crinosomes per all GFP-positive granules in −6 h versus 0 h RPF glands; $n$ = 12–30 cells (Mann–Whitney $U$ test). In the box plots, bars show the data ranging between the upper and lower quartiles, and median is indicated as a horizontal black line within the box. Whiskers plot the smallest and largest observations.

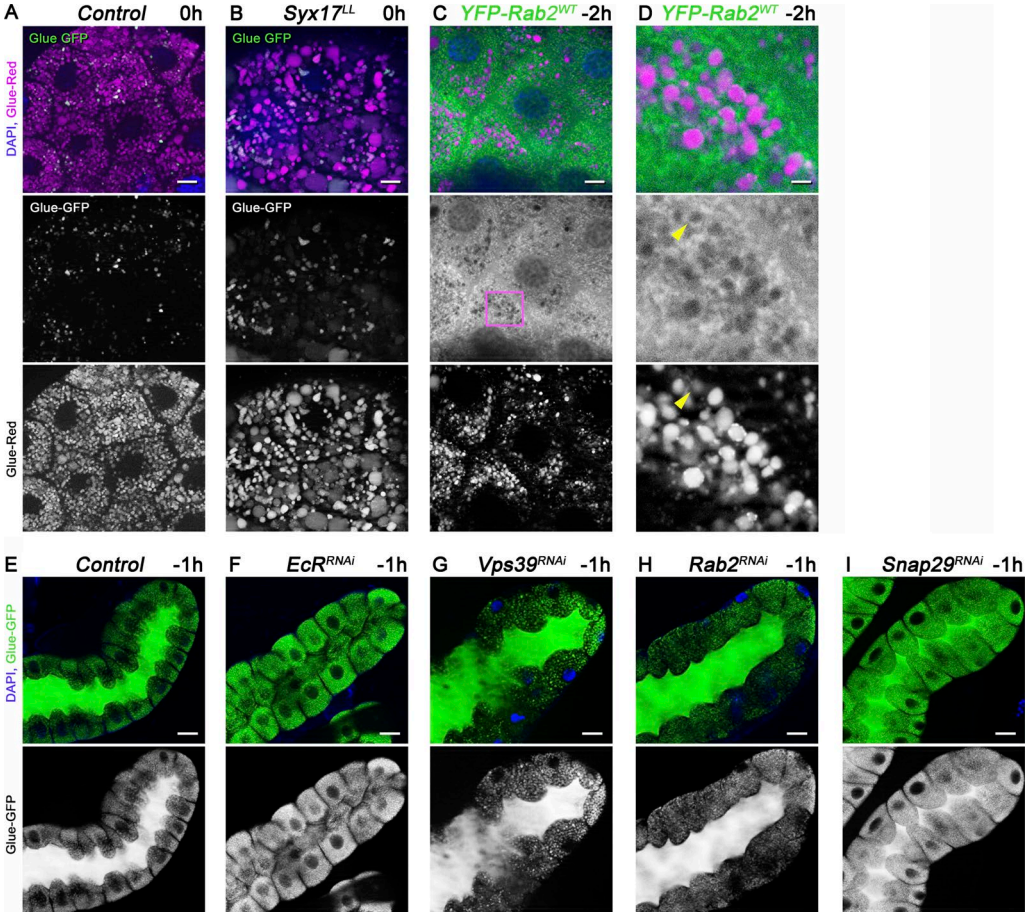


Figure S5. **Additional Syntaxin 17, YFP-Rab2, and glue secretion data.** (A and B) Glue granule degradation in white prepupal (0 h) salivary glands. (A) The majority of glue granules lack GFP signal in control cells. (B) Null mutation of *Syx17* does not prevent the crinophagic quenching of Glue-GFP. (C and D) The wild-type form of Rab2 is rarely detected in the limiting membrane of Glue-Red granules (C). The boxed region is shown enlarged in D, and the arrowhead points to a faint Rab2 ring surrounding a Glue-Red structure. (E–I) Crinophagy is dispensable for glue secretion. Large amounts of Glue-GFP are seen in the lumen of control salivary glands at −1 h RPF (E) and also in glands undergoing *Vps39* (G), *Rab2* (H), and *Snap29* (I) RNAi, unlike in the case of *EcR* knockdown (F), which prevents glue secretion. Green and/or magenta channels of merged images are shown separately in A–I. Bars: (A–C) 20 µm; (D) 3 µm; (E–I) 40 µm.

**Provided online is Table S1 in Excel, showing the effect of Qa SNARE inhibitions on the quenching of Glue-GFP. The effect of salivary gland cell–specific UAS-RNAi knockdown of genes encoding Qa SNAREs and the null mutant *Syntaxin 17*$^{LL06330}$ was tested on quenching of Glue-GFP in white prepupae (0 h RPF). Results are shown in the last column, and the first column displays the human homologues of these genes.**